AIP | APL Materials

Kinetics versus thermodynamics of the metal incorporation in molecular beam epitaxy of (InxGa1−x)2O3

Patrick Vogt and Oliver Bierwagen

Citation: APL Mater. **4**, 086112 (2016); doi: 10.1063/1.4961513
View online: http://dx.doi.org/10.1063/1.4961513
View Table of Contents: http://scitation.aip.org/content/aip/journal/aplmater/4/8?ver=pdfcov
Published by the AIP Publishing

Kinetics versus thermodynamics of the metal incorporation in molecular beam epitaxy of $(In_xGa_{1-x})_2O_3$

Patrick Vogt[a] and Oliver Bierwagen[b]
Paul-Drude-Institut für Festkörperelektronik, Hausvogteiplatz 5–7, D-10117 Berlin, Germany

(Received 20 July 2016; accepted 10 August 2016; published online 23 August 2016)

We present a detailed study of the reaction kinetics and thermodynamics of the plasma-assisted oxide molecular beam epitaxy of the ternary compound $(In_xGa_{1-x})_2O_3$ for $0 \leq x \leq 1$. We measured the growth rate of the alloy *in situ* by laser reflectrometry as a function of growth temperature T_G for different metal-to-oxygen flux ratios r_{Me}, and nominal In concentrations x_{nom} in the metal flux. We determined *ex situ* the In and Ga concentrations in the grown film by energy dispersive X-ray spectroscopy. The measured In concentration x shows a strong dependence on the growth parameters T_G, r_{Me}, and x_{nom} whereas growth on different co-loaded substrates shows that in the macroscopic regime of $\sim\mu m^3$ x does neither depend on the detailed layer crystallinity nor on crystal orientation. The data unveil that, in presence of In, Ga incorporation is kinetically limited by Ga_2O desorption the same way as during Ga_2O_3 growth. In contrast, In incorporation during ternary growth is thermodynamically suppressed by the presence of Ga due to stronger Ga–O bonds. Our experiments revealed that Ga adatoms decompose/etch the In–O bonds whereas In adatoms do not decompose/etch the Ga–O bonds. This result is supported by our thermochemical calculations. In addition we found that a low T_G and/or excessively low r_{Me} kinetically enables In incorporation into $(In_xGa_{1-x})_2O_3$. This study may help growing high-quality ternary compounds $(In_xGa_{1-x})_2O_3$ allowing band gap engineering over the range of 2.7–4.7 eV. [http://dx.doi.org/10.1063/1.4961513]

The transparent (semi)conducting oxide, indium sesquioxide In_2O_3, has been for decades a well studied material and reached industrial significance due to its good transparency in the visible regime of light and quite large band gap of $E_g = (2.7 \pm 0.1)$ eV.[1] In contrast, gallium sesquioxide Ga_2O_3 is a transparent semiconducting oxide and a rather new material. Due to its direct large band gap of $E_g = (4.7 \pm 0.2)$ eV,[2] it is transparent up to the deep ultra-violet (DUV) regime of light and a suitable material for DUV detectors and power devices with higher breakdown voltage and efficiency than SiC and GaN,[2] for instance. Alloying both materials into $(In_xGa_{1-x})_2O_3$ should enable to widen the wavelength range for DUV detectors and the growth of heterostructures.[3]

The applications mentioned above and the control of the compound concentration require a high degree of purity and crystallinity, that can be achieved by plasma-assisted oxide molecular beam epitaxy (MBE).[4–9]

So far, theoretical reports have predicted the miscibility of In_2O_3 and Ga_2O_3.[10–12] Experimental studies about the crystal structure and optical properties of $(In_xGa_{1-x})_2O_3$ grown by MBE,[13] pulsed laser deposition,[14,15] and metal-organic vapor phase epitaxy (MOVPE)[16,17] were carried out. For the latter method, it has been shown that no In was incorporated at too low O pressures in the growth chamber,[16] and that In likely has a tendency to float on the growth surface.[17] However, systematic

[a]Electronic mail: vogt@pdi-berlin.de
[b]Electronic mail: bierwagen@pdi-berlin.de

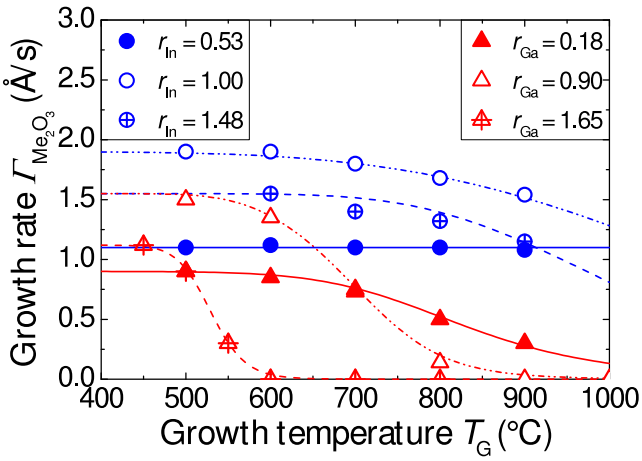

FIG. 1. Growth rate Γ of the binary oxides In_2O_3 (discs) and Ga_2O_3 (triangles) as a function of growth temperature T_G. The In flux for In_2O_3 growth was set to $\Phi_{In} = 1.00$ Å/s (filled), 1.90 Å/s (open), and 2.80 Å/s (crossed). The Ga flux for Ga_2O_3 growth was set to $\Phi_{Ga} = 0.90$ Å/s (filled), 1.55 Å/s (open), and 2.80 Å/s (crossed). The lines are guides to the eye. Data partly published in Ref. 6.

investigations of the reaction kinetics and studies of the In and Ga incorporation for the $(In_xGa_{1-x})_2O_3$ growth are lacking.

For the binary oxides In_2O_3 and Ga_2O_3, we have already shown that the growth rate Γ decreases in the Me-rich regime due to the oxygen-deficiency-induced formation of the volatile suboxide Me_2O (Me = In,Ga).[4–6] At high growth temperatures T_G Γ also decreases because of Me_2O desorption in the Me-rich and O-rich regimes. This decrease of Γ is stronger with increasing T_G for a larger Me-to-O flux ratio $r_{In,Ga} = \Phi_{In,Ga}/\Phi_O$ (see Fig. 1 and Refs. 5 and 6). The In, Ga, and active O fluxes are denoted as Φ_{In}, Φ_{Ga}, and Φ_O, respectively.

In this letter, we present a systematic study of the In and Ga incorporation into the ternary oxide $(In_xGa_{1-x})_2O_3$ as a function of T_G for different Me-to-O flux ratios $r_{Me} = (\Phi_{In} + \Phi_{Ga})/\Phi_O$ ranging from 0.1 to 2.0, and In-to-Ga flux ratios $x_{nom} = \Phi_{In}/(\Phi_{In} + \Phi_{Ga})$ ranging from 0 to 1. The results are discussed in terms of kinetic and thermodynamic limitations. Growth conditions to force metal incorporation are demonstrated as well. However, the miscibility of In_2O_3 and Ga_2O_3 as well as the crystallinity of $(In_xGa_{1-x})_2O_3$ are beyond the scope of this study.

The samples were grown in a custom made MBE system equipped with a laser-reflectometry set-up (LR) that allows the *in-situ* measurement of Γ and a line-of-sight quadrupole mass spectrometer (QMS) that also allows to monitor *in-situ* the actual desorbing flux from the substrate.[4] Standard shuttered hot-lip effusion cells were used to evaporate liquid In and Ga (7N purity). The beam equivalent pressure (BEP) which is proportional to the particle flux was measured by a nude filament ion gauge positioned at the substrate location.

The Me fluxes were calibrated by measuring Γ of the In_2O_3 and Ga_2O_3 layers in the O-rich regime at sufficiently low T_G where neither Me_2O desorption nor Me accumulation occurs.[4–6] With this calibration we converted the measured BEPs into equivalent Me_2O_3 growth rates that are used throughout this study.

A radio frequency plasma source with a mass flow controller supplied Φ_O from the research-grade O_2 gas (6N purity). The radio frequency power of the plasma source was maintained at 300 W. The O_2 mass flows Φ_{O_2} were set to 0.5, 1.0, and 2.0 standard cubic centimeter per minute (SCCM). Due to the different oxidation efficiencies of In[4] and Ga,[4] Φ_O was calculated for all values of x_{nom} as

$$\Phi_O = \Phi_{O_2}\left(x_{nom}\,\Phi_O^{In} + (1 - x_{nom})\,\Phi_O^{Ga}\right) \quad (1)$$

with $\Phi_O^{In} = \Phi_O(x_{nom} = 1) = 5.7$ Å/(s × SCCM) and $\Phi_O^{Ga} = \Phi_O(x_{nom} = 0) = 1.7$ Å/(s × SCCM) determined from the growth at stoichiometric condition of the binary oxide In_2O_3 and Ga_2O_3, respectively.[4] Table I summarizes the growth parameters employed throughout this study.

TABLE I. Growth parameters and corresponding figure symbols in Figs. 1–4 for the $(In_xGa_{1-x})_2O_3$ growth.

Figure symbols	r_{Me}	x_{nom}	Φ_{In} (Å/s)	Φ_{Ga} (Å/s)	Φ_O (Å/s)
Centered (inset in Fig.)	0.10	0.50	0.50	0.50	10.80
Filled	0.47	0.45	1.44	1.81	6.82
Open	0.72	0.70	1.12	1.60	3.20
Dotted	0.75	0.25	0.50	1.50	2.65
Crossed	2.00	0.50	1.80	1.80	1.80

Using QMS, T_G was calibrated by monitoring the total reflection of a known Φ_{Ga} desorbing from an Al_2O_3 (0001) surface. In order to obtain T_G, we slowly decreased the thermo-couple temperature of the substrate heater T_{TC} until Me atoms started adsorbing on the substrate. Besides, T_G was calculated by applying kinetic theory of gases as reported in Ref. 18 that enabled determining the offset between T_{TC} and T_G ($\Delta T = T_{TC} - T_G$).

Depending on T_G, r_{Me}, and x_{nom} the layers were either amorphous, polycrystalline, or crystalline. The In layer concentration x was obtained by measuring a macroscopic volume of the epilayer of ~4 μm^3 in a scanning electron microscope by means of energy dispersive X-ray spectroscopy (EDX).

In order to investigate whether x depends on the substrate material and orientation, different cleaved substrates of Al_2O_3 ((0001),(11$\bar{2}$0),(10$\bar{1}$2)) and Y-stabilized ZrO_2 (YSZ)((111),(100)) were In-bonded on a Si wafer and the $(In_xGa_{1-x})_2O_3$ layers were grown simultaneously on different substrates. It turned out that at a scale of a macroscopic volume x neither depends on the substrate material and orientation, nor on the crystallinity of the film. The crystallinity and structure of the alloys were identified *in-situ* by reflection high energy electron diffraction during growth and *ex-situ* by X-ray diffraction ω-2θ wide-range scans (not shown).

Figure 1 shows the measurement of Γ of the binary grown In_2O_3 and Ga_2O_3 as a function of T_G. The dependencies of Γ on T_G for both materials are discussed in detail in Refs. 5 and 6. The stronger decrease of $\Gamma_{Ga_2O_3}$ with T_G and $r_{Ga} = \Phi_{Ga}/\Phi_O$ is kinetically explained by the higher vapor pressure of its suboxide Ga_2O as compared to the suboxide In_2O.[6]

Figure 2 depicts Γ of the ternary film $\Gamma_{(In_xGa_{1-x})_2O_3}$ for x_{nom} = 0.25, 0.45, 0.50, and 0.70 at different r_{Me} as a function of T_G. Similar to the growth of the binary oxides depicted in Fig. 1 and reported in Refs. 5 and 6, lowering r_{Me} extends the growth domain of $(In_xGa_{1-x})_2O_3$ towards higher T_G. This can be seen by comparing Γ for x_{nom} = 0.5 and r_{Me} = 0.1, 2.0, for instance. Particularly, for the lowest r_{Me} = 0.1 (inset, Fig. 2) we do not observe any decrease of Γ up to T_G = 800 °C.

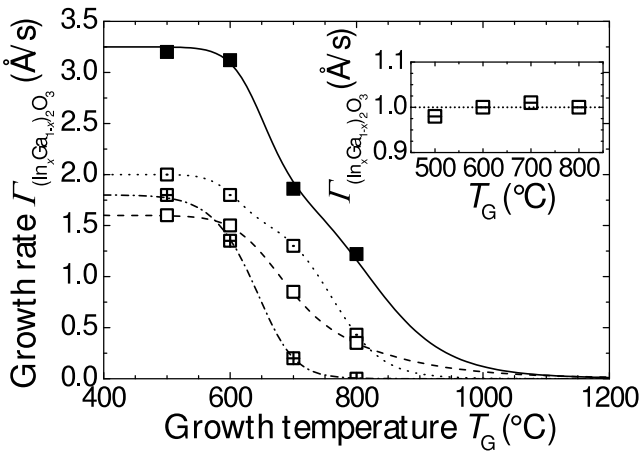

FIG. 2. Growth rate of $(In_xGa_{1-x})_2O_3$ $\Gamma_{(In_xGa_{1-x})_2O_3}$ as a function of growth temperature T_G plotted for different r_{Me} = 0.47, 0.72, 0.75, 2.00 and x_{nom} = 0.45, 0.70, 0.25, 0.50 for filled, open, dotted, and crossed squares, respectively (see Table I). Inset: $\Gamma_{(In_xGa_{1-x})_2O_3}$ as a function of T_G for r_{Me} = 0.1 and x_{nom} = 0.50 (centered squares). The lines are guides to the eye.

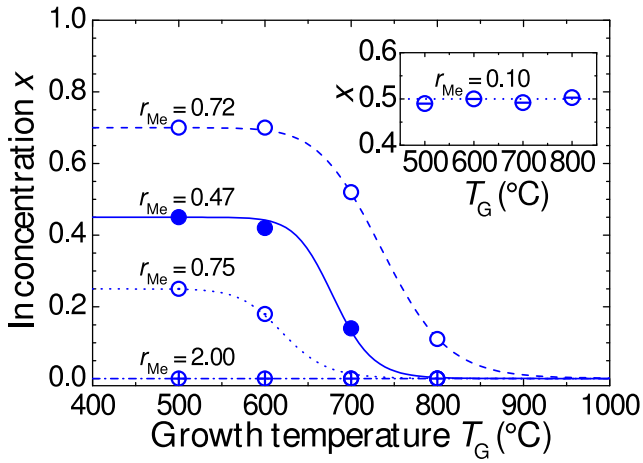

FIG. 3. In concentration x as a function of growth temperature T_G plotted for different r_{Me} and x_{nom} (see Table I). Inset: x versus T_G for $r_{Me} = 0.10$ (centered discs). The lines are guides to the eye.

In order to unveil the relative loss of In and Ga contributing to the decrease of $\Gamma_{(In_xGa_{1-x})_2O_3}$ with T_G, we investigated x as a function of T_G for the growth conditions indicated in Table I. The results are plotted in Fig. 3. Under O-rich growth conditions of $r_{Me} < 1.0$ and $T_G < 600\,°C$ $x = x_{nom}$. For $T_G \leq 600\,°C$ x decreases with increasing T_G for $0.1 < r_{Me} < 1.0$. However, for $r_{Me} \leq 0.1$, x does not depend on T_G up to 800 °C and is equal to x_{nom} (inset, Fig. 3). Under Me-rich growth conditions, for $r_{Me} = 2.0$ and $\Phi_O = \Phi_{In} = \Phi_{Ga}$, $x = 0$ for all measured T_G, i.e., only Ga_2O_3 is formed. Scanning electron microscopy and EDX measurements revealed that In accumulated as droplets on the growth surface for this sample at $T_G < 600\,°C$ (not shown). Similar metal accumulation has been observed during MBE under metal-rich growth conditions at these low T_G for In_2O_3 but not for Ga_2O_3.[6] This finding suggests preferential incorporation of Ga over In.

Now, we focus on the growth experiments of $(In_xGa_{1-x})_2O_3$ for which x_{nom} was set to 0.5 and 0.45 and discuss the individual incorporation rates of In and Ga into $(In_xGa_{1-x})_2O_3$. In order to access these quantities we introduce pseudo-binary growth rates γ defined as

$$\gamma_{In_2O_3} = x\Gamma_{(In_xGa_{1-x})_2O_3} \tag{2}$$

and

$$\gamma_{Ga_2O_3} = (1-x)\Gamma_{(In_xGa_{1-x})_2O_3}. \tag{3}$$

Figure 4 depicts the variation of $\gamma_{In_2O_3}$ and $\gamma_{Ga_2O_3}$ as a function of T_G. Note that the definitions of $\gamma_{In_2O_3}$ and $\gamma_{Ga_2O_3}$ do not take into account the difference in cation densities due to different possible crystal phases during $(In_xGa_{1-x})_2O_3$ growth. Therefore, we assume a maximum error of $\gamma_{In_2O_3}$ and $\gamma_{Ga_2O_3}$ of $\delta\gamma = \pm 10\,\%$ based on the difference in cation densities of bixbyite In_2O_3 and monoclinic Ga_2O_3. This difference, however, does not change the qualitative evolution of γ as a function of T_G. The evolution of $\gamma_{Ga_2O_3}$ follows the same trend as the one for $\Gamma_{Ga_2O_3}$ plotted in Fig. 1. In contrast, $\gamma_{In_2O_3}$ is strongly reduced for $T_G > 600\,°C$ and $r_{Me} > 0.1$ compared to the binary $\Gamma_{In_2O_3}$ depicted in Fig. 1. However, the inset shows a constant γ at $r_{Me} = 0.1$ for both materials up to $T_G = 800\,°C$.

Based on the data plotted in Figs. 2–4, we can define a range of r_{Me} where x decreases with T_G,

$$0.1 < r_{Me} < 2.0. \tag{4}$$

For $r_{Me} \leq 0.1$ (inset in Figs. 2–4 for $r_{Me} = 0.1$) all In is incorporated, whereas, for $r_{Me} \geq 2.0$ (crossed symbols in Figs. 2–4 for $r_{Me} = 2.0$) no In incorporation could be measured.

Our results strongly suggest that the presence of Ga inhibits the incorporation of In whereas the presence of In has no qualitative effect on Ga incorporation. However, considering kinetic factors, one would expect incorporation of In to be higher than that of Ga since the oxidation efficiency of In into In_2O_3 is higher than that of Ga into Ga_2O_3 and the vapor pressure of In_2O is lower than the

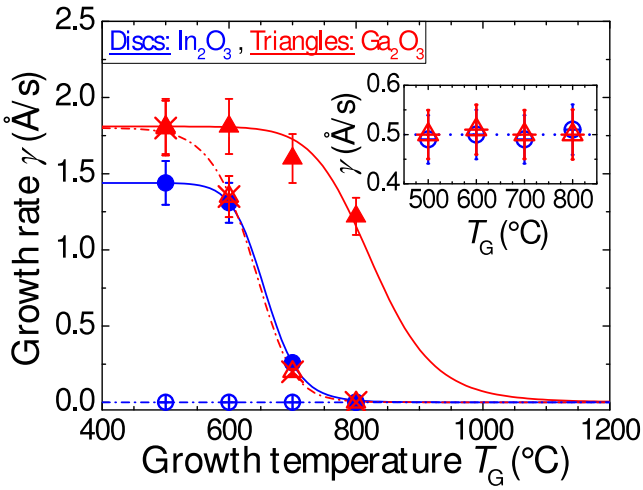

FIG. 4. The pseudo-binary growth rates γ for In_2O_3 (discs) and Ga_2O_3 (triangles) from the ternary compound $(In_xGa_{1-x})_2O_3$ (Figs. 2 and 3) as a function of growth temperature T_G are depicted for $x_{nom} \sim 0.5$ (see text). The symbols correspond to growth parameters indicated in Table I. The lines are guides to the eye.

one of Ga_2O. To explain the contradicting results between Γ of the binary grown In_2O_3 and Ga_2O_3, and γ derived from the ternary growth, we suggest the suppressed In incorporation could be of thermodynamic origin since the Ga–O bond energy is higher than the In–O bond energy, as calculated by first-principles density functional calculations.[19] We verify this hypothesis in two ways: (i) We did complementary etch-experiments to try to decompose the In–O and Ga–O bonds with Ga and In, respectively. (ii) We performed thermochemical calculations (see the supplementary material).

In a former publication we have already shown that In_2O_3 and Ga_2O_3 layers can be etched (i.e., decomposed into Me_2O which then may desorb off or diffuse on the growth surface) by In and Ga, respectively.[4] In the present etch-experiment, we exposed the In_2O_3 layer to Φ_{Ga}, and reciprocally, the Ga_2O_3 layer to Φ_{In}, to see if one of the metals decomposes the oxide layer. Potential decomposition reactions read as

$$6\mathrm{Ga}\,(a) + \mathrm{In_2O_3}\,(s) \rightarrow 3\mathrm{Ga_2O}\,(g) + 2\mathrm{In}\,(a \text{ or } g)\,, \quad (5)$$

$$4\mathrm{Ga}\,(a) + \mathrm{In_2O_3}\,(s) \rightarrow 2\mathrm{Ga_2O}\,(g) + \mathrm{In_2O}\,(a \text{ or } g)\,, \quad (6)$$

$$6\mathrm{In}\,(a) + \mathrm{Ga_2O_3}\,(s) \rightarrow 3\mathrm{In_2O}\,(g) + 2\mathrm{Ga}\,(a \text{ or } g)\,, \quad (7)$$

$$4\mathrm{In}\,(a) + \mathrm{Ga_2O_3}\,(s) \rightarrow 2\mathrm{In_2O}\,(g) + \mathrm{Ga_2O}\,(a \text{ or } g)\,, \quad (8)$$

where a, g, and s denote the adsorbate, gaseous, and solid phase, respectively. During the exposure of an In_2O_3 layer to Φ_{Ga}, the desorption of Ga_2O was detected by QMS and the intensity of the reflected laser signal changed. These results indicate that reactions (5) and/or (6) occurred. In contrast, In did not etch the Ga_2O_3 layer, as only desorbing In atoms were detected by QMS and the intensity of the detected laser signal remained constant. These observations indicate that reactions (7) and (8) did not take place.

Furthermore, our thermochemical calculations yield a negative Gibbs free enthalpy ΔG for reactions (5) and (6) and a positive one for reactions (7) and (8) (see the supplementary material for more details). Therefore reactions (5) and (6) should be feasible and reactions (7) and (8) should be hindered.

Based on the results presented above we conclude that the incorporation of Ga into $(In_xGa_{1-x})_2O_3$ is thermodynamically favored compared to the one of In. Particularly, our etch-experiments indicate that during $(In_xGa_{1-x})_2O_3$ growth, already oxidized In may be replaced by Ga, resulting in a segregation of In at the growth surface. A similar phenomenon has already been reported for $(In_xGa_{1-x})_2O_3$ MOVPE growth where it is suggested that In floats on the growth surface.[17] Similarly, In segregation at the growth surface has been observed during MBE growth of $(In_xGa_{1-x})N$.[20] In case of $(In_xGa_{1-x})_2O_3$ MBE growth, In atoms segregate either as In droplets or In_2O which desorbs at elevated T_G, explaining

the decrease of x and $\gamma_{In_2O_3}$ with increasing T_G in Figs. 3 and 4. This explanation is in accordance with our observations that increasing Φ_O and/or x_{nom} for $r_{Me} < 1$ leads to a higher x at given T_G. We suggest that at higher Φ_O Ga adatoms may experience a higher diffusion barrier, and therefore, they may be already oxidized into Ga_2O_3 before etching the In–O bonds. This explanation holds also true for an increased x_{nom} since (statistically) more In atoms may be oxidized into In_2O_3 and are not decomposed by Ga adatoms leading to an increase of x at same T_G.

In summary, we have studied the metal incorporation during the plasma-assisted oxide molecular beam epitaxial growth of $(In_xGa_{1-x})_2O_3$. The metal fluxes, metal-to-oxygen ratios, and growth temperature were systematically changed in order to understand the competing In and Ga incorporation into $(In_xGa_{1-x})_2O_3$. During binary growth, the metal incorporation in In_2O_3 and Ga_2O_3 is kinetically limited by the suboxide desorption of In_2O and Ga_2O, respectively. During ternary growth the Ga incorporation is not affected by the presence of In adatoms and remains kinetically limited by Ga_2O desorption. In contrast, the In incorporation into $(In_xGa_{1-x})_2O_3$ is controlled by the presence of Ga.

Our experiments revealed that Ga atoms are more favorably incorporated in $(In_xGa_{1-x})_2O_3$ than In atoms. We conducted etch-experiments that revealed that the Ga–O bonds are stronger than the In–O bonds, and therefore, already oxidized In atoms may be reduced by Ga adatoms. These experiments unveil that the Ga incorporation is thermodynamically favored compared to In incorporation, as also supported by our thermochemical calculations. Furthermore, we found that In either accumulates as droplets at the growth surface for growth temperatures below 600 °C or desorbs eventually as In or In_2O for growth temperatures above 600 °C. However, excess of oxygen kinetically enables (full) In incorporation for all investigated growth temperatures in the range from 500 °C to 800 °C. The thermodynamically favored Ga incorporation and kinetically enabled In incorporation likely also explains the different In incorporation rates at low and high O-pressures observed during metal-organic vapor phase epitaxy[17] and pulsed laser deposition[14] of $(In_xGa_{1-x})_2O_3$. Our findings may help growing high-quality $(In_xGa_{1-x})_2O_3$ layers with desired In and Ga concentrations. They may also constitute a qualitative guidance for the growth of $(In_xGa_{1-x})_2O_3$ by ozone molecular beam epitaxy, pulsed laser deposition, and metal-organic vapor phase epitaxy.

See supplementary material for thermochemical calculations of the given reactions.

We would like to thank Caroline Chèze for critically reading the manuscript, Hans-Peter Schönherr for technical MBE support, as well as Uwe Jahn and Anjneya Verma for EDX assistance. In addition, we would like to thank Caroline Chèze, Lutz Geelhaar, Henning Riechert, Martin Albrecht, Oliver Brandt, and Raffaella Calarco for fruitful discussions. The publication of this article was partly funded by the open access fund of the Leibniz Association.

[1] O. Bierwagen, Semicond. Sci. Technol. **30**, 024001 (2015).
[2] M. Higashiwaki, K. Sasaki, H. Murakami, Y. Kumagai, A. Koukitu, A. Kuramata, T. Masui, and S. Yamakoshi, Semicond. Sci. Technol. **31**, 034001 (2016).
[3] S. Fujita and K. Kaneko, J. Cryst. Growth **401**, 588 (2014).
[4] P. Vogt and O. Bierwagen, Appl. Phys. Lett. **106**, 081910 (2015).
[5] P. Vogt and O. Bierwagen, Appl. Phys. Lett. **108**, 072101 (2016).
[6] P. Vogt and O. Bierwagen, Appl. Phys. Lett. **109**, 062103 (2016).
[7] P. Vogt, A. Trampert, M. Ramsteiner, and O. Bierwagen, Phys. Status Solidi A **212**, 1433 (2015).
[8] K. Sasaki, M. Higashiwaki, A. Kuramata, T. Masui, and S. Yamakoshi, J. Cryst. Growth **392**, 30 (2014).
[9] T. Oshima, T. Okuno, and S. Fujita, Jpn. J. Appl. Phys. **46**, 7217 (2007).
[10] H. Peelaers, D. Steiauf, J. B. Varley, A. Janotti, and C. G. Van de Walle, Phys. Rev. B **92**, 085206 (2015).
[11] M. B. Maccioni, F. Ricci, and V. Fiorentini, J. Phys.: Conf. Ser. **566**, 012016 (2014).
[12] M. B. Maccioni, F. Ricci, and V. Fiorentini, Appl. Phys. Express **8**, 021102 (2015).
[13] T. Oshima and S. Fujita, Phys. Status Solidi C **5**, 3113 (2008).
[14] H. V. Wenckstern, D. Splith, M. Purfürst, Z. Zhang, C. Kranert, S. Müller, M. Lorenz, and M. Grundmann, Semicond. Sci. Technol. **30**, 024005 (2015).
[15] C. Kranert, J. Lenzner, M. Jenderka, M. Lorenz, H. von Wenckstern, R. Schmidt-Grund, and M. Grundmann, J. Appl. Phys. **116**, 013505 (2014).
[16] M. Baldini, D. Gogova, K. Irmscher, M. Schmidbauer, G. Wagner, and R. Fornari, Cryst. Res. Technol. **49**, 552 (2014).
[17] M. Baldini, M. Albrecht, D. Gogova, R. Schewski, and G. Wagner, Semicond. Sci. Technol. **30**, 024013 (2015).
[18] R. Held, D. E. Crawford, A. M. Johnston, A. M. Dabiran, and P. I. Cohen, Surf. Rev. Lett. **5**, 913 (1998).
[19] H. K. Noh, K. J. Chang, B. Ryu, and W. J. Lee, Phys. Rev. B **84**, 1 (2011).
[20] Z. Deng, Y. Jiang, W. Wang, L. Cheng, W. Li, W. Lu, H. Jia, W. Liu, J. Zhou, and H. Chen, Sci. Rep. **4**, 6734 (2014).